IEEE Access
Multidisciplinary ⋮ Rapid Review ⋮ Open Access Journal

Received August 20, 2019, accepted August 30, 2019, date of publication September 6, 2019, date of current version September 20, 2019.

Digital Object Identifier 10.1109/ACCESS.2019.2939913

Optimal Operation Strategy of Multi-Energy Complementary Distributed CCHP System and Its Application on Commercial Building

QINGHUA WANG[1], JIZHEN LIU[1,2], YANG HU[2], AND XIAONING ZHANG[2]
[1]State Key Laboratory of Alternate Electrical Power System With Renewable Energy Sources, North China Electric Power University, Beijing 102206, China
[2]School of Control and Computer Engineering, North China Electric Power University, Beijing 102206, China

Corresponding author: Yang Hu (hooyoung@ncepu.edu.cn)

This work was supported in part by the National Natural Science Foundation of China under Grant 51676068, in part by the National Science and Technology Major Project under Grant 2017-V-0010-0061, and in part by the Fundamental Research Funds for the Central Universities under Grant 2019MS024.

ABSTRACT For distributed energy system, multi-energy sources and their comprehensive utilization are popularly concerned nowadays. In this paper, optimal operation of a multi-energy complementary distributed combined cooling, heating and power (CCHP) system is deeply studied. This system is applied on a commercial building in Beijing and it has complex configuration including natural gas energy source, renewable energy source and different energy conversion devices. Meanwhile, a separated cooling, heating and power (SCHP) supply system is also proposed. Their optimal operation strategies and performance are compared to show the advantages of multi-energy complementary system. Through simulation, the results show that the multi-energy complementary system operates with great performance and the optimal operation strategy is effective.

INDEX TERMS Combined cooling, heating and power system, distributed energy system, multi-energy complementary system, optimal operation.

I. INTRODUCTION

Multi-energy complementary distributed combined cooling, heating and power (CCHP) system integrates micro-turbine, renewable power generators, energy storage system, heat recovery system and refrigeration equipment as a whole to realize complementary utilization of multi-energy sources. Energy conversion efficiency, economic and environmental impacts of the multi-energy complementary CCHP system largely depend on the system structure, optimal objectives and operation strategies. Grounded in the fast development of distributed energy system (DES) and energy storage technology, the concept of multi-energy complementary becomes tractable and is attracting increasing amounts of attentions for its capability of utilizing stochastic renewable energy and raising the energy utilization efficiency.

One of the fundamental problems in fully harnessing the potential of multi-energy complimentary CCHP system is the determination of system configuration. A CCHP system normally consists of prime movers (e.g., gas turbine, Stirling engine and fuel cell), renewable power generators (e.g., wind turbine and solar photovoltaic) and auxiliary equipment (e.g., organic Rankine cycle (ORC) and refrigeration equipment). Two beta type Stirling engines [1] were suggested in the CCHP system to analyze the energy flow of the absorption chiller by utilizing waste heat of the engine. In [2]–[4], the optimal planning and operation strategies of a CCHP system that includes renewable energy and other distributed generators were discussed to reduce the total cost and CO_2 emissions. Besides, auxiliary equipment can be adopted in the new CCHP systems to improve performance coefficient. A complementary ORC system [5], [6] was added to CCHP system, which enabled an adjustable electricity to thermal energy output ratio via changing the loads of ORC dynamically. A structural configuration of the CCHP system with hybrid chillers was proposed in [7], [8], consisting of a combined electric and absorption chiller, whose electric cooling to cool load ratio varied according to different electric and thermal loads in every hour. However, impacts of auxiliary equipment on the system exist in various aspects and the

The associate editor coordinating the review of this manuscript and approving it for publication was Khmaies Ouahada.

intrinsic association between system components have not been investigated.

For a multi-energy system with specific configuration, optimizing energy utilization is a critical problem. Based on different performance criteria, various optimal operation strategies have been developed and implemented. Research in [9] proposed a two-stage multi-objective scheduling method which included an optimal power flow calculation stage and a decision-making stage. Considering operational constraints of the electric distribution network, the natural gas network and energy centers were introduced for the optimal scheduling in [10], [11]. The stochastic multi-objective scheduling approach was used to consider the probabilistic constraints, caused by uncertainties of renewable energy resources and electric and/or heating loads. A mixed integer nonlinear programming model for a combined CCHP system coupled with renewable energy was presented in [12], [13] to determine the optimal structure, capacity and operation strategies. A novel optimized control strategy for improving the load-following capability of CHP units was developed in [11], [14], aiming to borrow the heat extraction output to follow fast load changes given that its influence in tens of minutes on heat consumers was slight owing to the large inertia of district heating networks. Evaluating the system is a major issue which is foundation of the discussion on optimization. The comprehensive performance criterion focusing on various aspects (e.g., economic, environmentally friendly) can better guide the system operation.

Operation optimization of a distributed system normally focuses on profit maximization or cost minimization. A multi-objective optimal hybrid power flow algorithm was presented in [15], [16] using intelligent algorithm (e.g., improved genetic algorithm, particle swarm optimization) to minimize the operation cost and total emissions of the integrated local area energy systems. According to the grid-connected requirements of wind power and the capability of distributed battery energy storage system to damp power fluctuation, an optimized model was established in [17] with the objectives to minimize operation cost and maximize wind power integration. Optimal operation of CCHP system equipped with solar photovoltaic and photothermic (PV/PT) integrated module was discussed in respects of economy, energy consumption and environment. In order to achieve energy saving and emission reduction, a multi-energy complementary distributed energy system in [18] was designed integrating wind power and photovoltaic power. The optimization algorithm should be adaptive to the demand and operation status. And system operation can be adjusted in time automatically.

As previously reviewed, different configurations of multi-energy systems have been studied and optimized. However, in practice, with the increase of energy-supply or energy-conversion devices, the methods become unsuitable for the current multi-energy complimentary CCHP systems. There is an urgent need for a strategy considering safety, sustainability and economy. The operation optimization should reflect the internal mechanism and states of the system when the operating strategy changes. Main purpose of the paper is to realize the optimal operation of a commercial building with complex configuration including natural gas energy source, renewable energy source and different energy-conversion devices. More concretely, main contributions of this paper are listed as follows:

- A multi-energy complementary distributed CCHP system is established. The interactions between demand load, system structure and installed capacity in various operation scenarios are proposed in detail.
- The comprehensive performance evaluation considering the primary energy consumption, CO_2 emissions and operation cost is presented. And the optimal operation strategy to this multi-energy complementary distributed CCHP system is developed.
- Through comparison to a SCHP supply system, impacts of complementary equipment on safety, sustainability and economy are discussed.

The rest of this paper is organized as follows. Section II introduces the scenario description and task modes of a multi-energy complementary distributed CCHP system. Section III discusses the operation strategy and evaluation method of the system. Simulation and validation are studied in Section IV. Section V concludes this paper.

II. SCENARIO DESCRIPTION AND TASK MODES

A. DESCRIPTION OF MULTI-ENERGY COMPLEMENTARY DISTRIBUTED CCHP SYSTEM

For the application on commercial buildings, a typical solution is defined in Figure 1 where the distributed CCHP system is formed considering multi-energy complementary.

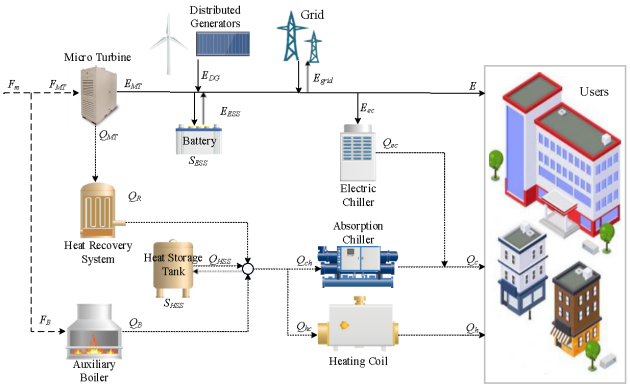

FIGURE 1. Flow chart of typical multi-energy complementary distributed CCHP system.

E, Q_c and Q_h are the electric, cooling and heating loads of users. F_m, F_{MT} and F_B are the fuel consumption of whole system, micro gas turbine and auxiliary boiler. E_{MT} and E_{DG} are the output power of micro gas turbine and distributed renewable power generation units. E_{ESS} and E_{grid} are the transmitted electricity by battery and power grid. E_{ec} is the electricity consumption of electric chiller. Q_{MT}, Q_R, Q_{HSS},

Q_B and Q_{ec} are the heat provided by micro gas turbine, heat recovery system, heat storage tank, auxiliary boiler and electric chiller. S_{ESS} and S_{HSS} are the energy state of battery and heat storage tank at time t.

If equipment capacity and installed structure have been determined, optimal operation is needed to track the multiple and stochastic loads utilizing the controllable or random primary energy sources. For ease of analysis, the following assumptions are made:

a. The energy supply and conversion devices can operate at any point within its rated capacity.
b. Efficiency of the devices remains unchanged at any operating point.
c. Energy losses in the transmission are neglected.

In Figure 1, the electric power conservation equation is:

$$E_{MT} + E_{DG} + E_{ESS} + E_{grid} = E + E_{ec} \quad (1)$$

$$E_{ESS} = S_{ESS_{t+1}} - S_{ESS_t} \quad (2)$$

where $E_{grid} < 0$ and $E_{grid} \geq 0$ mean power selling and purchasing with power grid, $E_{ESS} \geq 0$ and $E_{ESS} < 0$ mean battery charging and discharging, S_{ESS_t} means the charge-capacity at time t. Other terms in (1) are defined above.

Define the surplus power E_n as following:

$$E_n = E_{MT} + E_{DG} - E - E_{ec} \quad (3)$$

If $E_n \geq 0$, it reflects that surplus power exists, to charge the battery or be sold to power grid. If $E_n < 0$, it suggests that the CCHP system needs battery discharge or power purchase from power grid to make up the electricity shortage. The heat power conservation equation is:

$$Q_R + Q_{HSS} + Q_B = Q_{ch} + Q_{hc} \quad (4)$$

$$Q_{HSS} = S_{HSS_{t+1}} - S_{HSS_t} \quad (5)$$

$$Q_c = Q_{ec} + Q_{ch}\eta_{ch} \quad (6)$$

$$Q_h = Q_{hc}\eta_{hc} \quad (7)$$

$$Q_c + Q_h = Q \quad (8)$$

where $Q_{HSS} \geq 0$ and $Q_{HSS} < 0$ means that the heat storage tank absorbs and releases heat.

Assume that the heat needed by absorption chiller to fulfill the whole cooling load is denoted by Q_{creq}, the heat needed by heating coil to fulfill the whole heating load is denoted by Q_{hreq}. They can be calculated by

$$Q_{creq} = \frac{Q_c}{\eta_{ch}} \quad (9)$$

$$Q_{hreq} = \frac{Q_h}{\eta_{hc}} \quad (10)$$

where the total heat is $Q_{req} = Q_{creq} + Q_{hreq}$.

B. FOLLOWING-ELECTRIC-LODA HEAT-SUPPLY MODE

The following-electric-load (FEL) heat supply mode requires priority to meet electric power load. For the multi-energy complementary structure in Figure 1, output power of micro-gas-turbine should be coordinated with the renewable power, which is pre-knowable via ultra-short term prediction, to fulfill electric power load firstly. Then, the surplus renewable power can be stored in the battery. Until it is charged to the maximum capacity state, the renewable power still surplus can be sold to the power grid.

If electric power load of the distributed CCHP system cannot be fulfilled, the electricity shortage will be preferentially supplied by the battery. Until it is discharged to the minimum capacity state and the electric power load still cannot be fulfilled, the lacked power can be purchased from the power grid.

The low-grade heat from micro-gas-turbine is recycled by the heat-recovery-system, to fulfill the cooling and heating loads. If the heat is too much and surplus after that, it can be stored in the heat-storage-tank. If the heat is not enough to fulfill the cooling and heating loads, the heat-storage-tank will provide heat. In case it is still useless, the heating load should be preferentially fulfilled whereas the absorption-chiller will be started to provide cooling load. In case the heating load is also insufficient, auxiliary-boiler will be started to provide heating load.

According to E_n, there are two cases under the FEL mode. The detail operation strategies of battery are shown as following:

a. When $E_n \geq 0$, battery charging is given priority until the battery is fully charged and the surplus electricity is sold to the power grid. For the charging state, there exist

$$\begin{cases} S_{ESS_{t+1}} = S_{ESS_t} + E_n \\ E_{grid} = 0 \end{cases} \quad S_{ESS_t} + E_n \leq S_{ESS,max} \quad (11)$$

For the fully charged state, there exist

$$\begin{cases} S_{ESS_{t+1}} = S_{ESS,max} \\ E_{grid} = S_{ESS_t} + E_n - S_{ESS,max} \end{cases} \quad S_{ESS_t} + E_n \geq S_{ESS,max} \quad (12)$$

b. When $E_n < 0$, battery is used to compensate the electricity shortage preferentially until the battery is fully discharged and the lacked electricity is bought from the power grid. For the discharging state, there exist

$$\begin{cases} S_{ESS_{t+1}} = S_{ESS_t} + E_n \\ E_{grid} = 0 \end{cases} \quad S_{ESS_t} + E_n > S_{ESS,min} \quad (13)$$

For the fully discharged state, there exist

$$\begin{cases} S_{ESS_{t+1}} = S_{ESS,min} \\ E_{grid} = S_{ESS_t} - S_{ESS,min} + E_n \end{cases} \quad S_{ESS_t} + E_n \leq S_{ESS,min} \quad (14)$$

Besides, in order to use the renewable power as much as possible, E_n is strongly determined by the relationship between renewable power supply and electric power load. Two cases and the detail operation strategies are discussed as following:

Case 1: The predicted renewable power exceeds the electrical load, $E_{DG} \geq E$.

a. When the thermal-energy in heat-storage-tank is enough to fulfill cooling and heating loads, there exist

$$S_{\mathrm{HSS}_t} - S_{\mathrm{HSS,min}} \geq Q_{\mathrm{req}} \tag{15}$$

Herein, the micro-gas-turbine, auxiliary boiler and absorption chiller do not start, so there exist $E_{\mathrm{n}} \geq 0$, $F_{\mathrm{m}} = 0$, $E_{\mathrm{ec}} = 0$ and

$$S_{\mathrm{HSS}_{t+1}} = S_{\mathrm{HSS}_t} - Q_{\mathrm{req}} \tag{16}$$

Besides, $S_{\mathrm{ESS}_{t+1}}$ and E_{grid} can be determined according to (11) and (12).

b. When the thermal-energy in heat-storage-tank only fulfill the heating load, there exist

$$\begin{cases} S_{\mathrm{HSS}_t} - S_{\mathrm{HSS,min}} < Q_{\mathrm{req}} \\ S_{\mathrm{HSS}_t} - S_{\mathrm{HSS,min}} \geq Q_{\mathrm{hreq}} \end{cases} \tag{17}$$

Herein, the heat-storage-tank fulfills the heating load firstly. The micro-gas-turbine and auxiliary boiler do not start. The absorption chiller starts to provide cooling load. Then, there exist $F_{\mathrm{m}} = 0$ and

$$E_{\mathrm{ec}} = \frac{Q_{\mathrm{c}} - \eta_{\mathrm{ch}} \left(S_{\mathrm{HSS}_t} - S_{\mathrm{HSS,min}} - Q_{\mathrm{hreq}}\right)}{\eta_{\mathrm{ec}}} \tag{18}$$

$$S_{\mathrm{HSS}_{t+1}} = S_{\mathrm{HSS,min}} \tag{19}$$

According to (3), $E_{\mathrm{n}} = E_{\mathrm{DG}} - E - E_{\mathrm{ec}}$ which may be positive or negative. Besides, $S_{\mathrm{ESS}_{t+1}}$ and E_{grid} can be determined according to (11)-(14).

c. When the thermal-energy in heat-storage-tank is not enough to fulfill the heating load, there exist

$$S_{\mathrm{HSS}_t} - S_{\mathrm{HSS,min}} < Q_{\mathrm{hreq}} \tag{20}$$

Herein, the micro-gas-turbine do not start while the auxiliary starts to make up the heating load and the electric chiller starts to provide the whole coling load. Then, there exist $S_{\mathrm{HSS}_{t+1}} = S_{\mathrm{HSS,min}}$, $E_{\mathrm{ec}} = Q_{\mathrm{c}}/\eta_{\mathrm{ec}}$ and

$$F_{\mathrm{m}} = \frac{Q_{\mathrm{hreq}} - \left(S_{\mathrm{HSS}_t} - S_{\mathrm{HSS,min}}\right)}{\eta_{\mathrm{B}}} \tag{21}$$

E_{n} is similar in that of b and so do $S_{\mathrm{ESS}_{t+1}}$ and E_{grid}.

Case 2: The predicted renewable power is less than the electric power load, $E_{\mathrm{DG}} < E$. The micro-gas-turbine starts to make up the electric power load. Moreover, if $E_{\mathrm{DG}} + E_{\mathrm{MT,max}} < E$, the battery needs to discharge or even buying electricity from power grid, shown as following:

$$E_{\mathrm{MT}} = \begin{cases} E - E_{\mathrm{DG}} & E - E_{\mathrm{DG}} \leq E_{\mathrm{MT,max}} \\ E_{\mathrm{MT,max}} & E - E_{\mathrm{DG}} > E_{\mathrm{MT,max}} \end{cases} \tag{22}$$

E_{n} may be positive or negative. The consumed fuel by micro-gas-turbine is $F_{\mathrm{MT}} = E_{\mathrm{MT}}/\eta_{\mathrm{MT}}$. The heat provided by the heat-recovery-system is $Q_{\mathrm{R}} = F_{\mathrm{MT}}(1 - \eta_{\mathrm{MT}})\eta_{\mathrm{R}}$.

a. When Q_{R} is enough to fulfill the cooling and heating loads, it means that $Q_{\mathrm{R}} \geq Q_{\mathrm{req}}$. Herein, the auxiliary boiler and electric chiller do not start, so $F_{\mathrm{m}} = F_{\mathrm{MT}}$ and $E_{\mathrm{ec}} = 0$. Output electric power from the micro-gas-turbine and renewable energy can properly fulfill the electric power load, so $E_{\mathrm{n}} = 0$, $E_{\mathrm{ESS}} = 0$ ($S_{\mathrm{ESS}_{t+1}} = S_{\mathrm{ESS}_t}$) and $E_{\mathrm{grid}} = 0$. The surplus thermal-energy from micro-gas-turbine is stored in the heat-storage-tank, shown as following

$$S_{\mathrm{HSS}_{t+1}} = \begin{cases} S_{\mathrm{HSS}_t} + Q_{\mathrm{R}} - Q_{\mathrm{req}} & \\ \qquad\qquad S_{\mathrm{HSS}_t} + Q_{\mathrm{R}} - Q_{\mathrm{req}} < S_{\mathrm{HSS,max}} & \\ S_{\mathrm{HSS,max}} \quad S_{\mathrm{HSS}_t} + Q_{\mathrm{R}} - Q_{\mathrm{req}} \geq S_{\mathrm{HSS,max}} & \end{cases} \tag{23}$$

b. When Q_{R} is not enough to fulfill the whole heat and cooling loads while the sum of thermal-energy provided by Q_{R} and the heat-storage-tank can fulfill the whole heating and cooling loads, there exists

$$\begin{cases} Q_{\mathrm{R}} < Q_{\mathrm{req}} \\ Q_{\mathrm{R}} + S_{\mathrm{HSS}_t} - S_{\mathrm{HSS,min}} \geq Q_{\mathrm{req}} \end{cases} \tag{24}$$

Herein, the auxiliary boiler and electric chiller do not start, so $F_{\mathrm{m}} = F_{\mathrm{MT}}$ and

$$S_{\mathrm{HSS}_{t+1}} = S_{\mathrm{HSS}_t} + Q_{\mathrm{R}} - Q_{\mathrm{req}} \tag{25}$$

Besides, output electric power from the micro-gas-turbine and renewable energy can properly fulfill electric power load, so $E_{\mathrm{n}} = 0$, $E_{\mathrm{ESS}} = 0$ ($S_{\mathrm{ESS}_{t+1}} = S_{\mathrm{ESS}_t}$) and $E_{\mathrm{grid}} = 0$.

c. When the thermal-energy provided by Q_{R} and the heat-storage-tank can only fulfill the heating load, there exists

$$\begin{cases} Q_{\mathrm{R}} + S_{\mathrm{HSS}_t} - S_{\mathrm{HSS,min}} < Q_{\mathrm{req}} \\ Q_{\mathrm{R}} + S_{\mathrm{HSS}_t} - S_{\mathrm{HSS,min}} \geq Q_{\mathrm{hreq}} \end{cases} \tag{26}$$

Herein, the auxiliary boiler does not start, so $F_{\mathrm{m}} = F_{\mathrm{MT}}$. The electric chiller is driven by E_{ec} to fulfill the cooling load, shown as following

$$E_{\mathrm{ec}} = \frac{Q_{\mathrm{c}} - \eta_{\mathrm{ch}}(Q_{\mathrm{R}} + S_{\mathrm{HSS}_t} - S_{\mathrm{HSS,min}} - Q_{\mathrm{hreq}})}{\eta_{\mathrm{ec}}} \tag{27}$$

Output electric power from micro-gas-wind turbine and renewable energy can properly fulfill the electric power load while $E_{\mathrm{ec}} \neq 0$, so $E_{\mathrm{n}} < 0$. Then, battery or power grid should provide the lacked power where $S_{\mathrm{ESS}_{t+1}}$ and E_{grid} can be determined according to (13)-(14).

d. When the thermal-energy provided by Q_{R} and the heat-storage-tank cannot fulfill the heating load, there exists

$$Q_{\mathrm{R}} + S_{\mathrm{HSS}_t} - S_{\mathrm{HSS,min}} < Q_{\mathrm{hreq}} \tag{28}$$

Herein, the auxiliary boiler starts to make up the heating load while the electric chiller starts to fulfill the whole cooling load. Then, there exists

$$F_{\mathrm{m}} = F_{\mathrm{MT}} + F_{\mathrm{B}} = F_{\mathrm{MT}} + \frac{Q_{\mathrm{hreq}} - Q_{\mathrm{R}} - \left(S_{\mathrm{HSS}_t} - S_{\mathrm{HSS,min}}\right)}{\eta_{\mathrm{B}}} \tag{29}$$

The heat-storage-tank is fully discharged, so $S_{\mathrm{HSS}_{t+1}} = S_{\mathrm{HSS,min}}$. Output electric power from the micro-gas-wind turbine and renewable energy can properly fulfill the electric power load while $E_{\mathrm{ec}} = Q_{\mathrm{c}}/\eta_{\mathrm{ec}} \neq 0$, so $E_{\mathrm{n}} < 0$. Then, the battery or power grid should provide the lacked electric power where $S_{\mathrm{ESS}_{t+1}}$ and E_{grid} can be determined according to (13)-(14).

C. FOLLOWING-THERMAL-LOAD POWER-SUPPLY MODE

The heat-load-followed (FTL) power-supply mode requires priority to meet heating and cooling loads of users. According to the sum of heating and cooling loads, output heat power of micro-gas-turbine is adjusted. If the required heating and cooling loads exceed the maximum output heat power of micro-gas-turbine, the heat-storage-tank will be used to make up the lacked heat power. If output heat power of micro-gas-turbine and heat-storage-tank cannot fulfill the total heating and cooling loads, the heating load should be preferentially fulfilled while the electric chiller should be started to make up the lacked cooling load. If output heat power of micro-gas-turbine and heat-storage-tank cannot fulfill the heating load, the auxiliary boiler should be started to make up the lacked heating load while the electric chiller should be started to make up the whole cooling load.

After determining the output heat power of micro-gas-turbine, its output electric power can be determined. Combined with the predicted renewable power, the surplus electric power can be calculated according to (3). If the surplus electric power exists meaning $E_{\mathrm{n}} \geq 0$, battery can be charged until it is full. The still surplus electric power can be sold to the power grid. If no surplus electric power exists meaning $E_{\mathrm{n}} < 0$, battery should preferentially supply electric power until it is empty. The still lacked electric power can be purchased from the power grid.

Under the FTL mode, whether E_{n} is positive cannot be determined due to the relationship between E and $E_{\mathrm{MT}}+E_{\mathrm{DG}}$ cannot be determined, so the cases $E_{\mathrm{n}} \geq 0$ and $E_{\mathrm{n}} < 0$ should be both discussed. $S_{\mathrm{ESS}_{t+1}}$ and E_{grid} should be calculated according to (11)-(14).

According to whether the whole cooling and heating loads can be fulfilled by the heat recovery system utilizing the produced heat from micro-gas-turbine, two cases can be obtained, carefully discussed as following:

Case 1: When the whole cooling and heating loads exceed the heat from heat recovery system utilizing the maximum heat power by micro-gas-turbine, there exist

$$Q_{\mathrm{req}} > Q_{R,\max} \tag{30}$$

$$F_{\mathrm{MT}} = F_{\mathrm{MT},\max} \tag{31}$$

a. If the heat produced by the heat recovery system and heat-storage-tank can fulfill the whole cooling and heating loads, there exists

$$Q_{R,\max} + S_{\mathrm{HSS}_t} - S_{\mathrm{HSS},\min} \geq Q_{\mathrm{req}} \tag{32}$$

Auxiliary boiler and electric chiller don't start, so $F_{\mathrm{m}} = F_{\mathrm{MT}}$ and $E_{\mathrm{ec}} = 0$. Besides, $S_{\mathrm{HSS}_{t+1}} = S_{\mathrm{HSS}_t} + Q_{\mathrm{R}} - Q_{\mathrm{req}}$.

b. If the heat produced by the heat recovery system and heat-storage-tank cannot fulfill the whole cooling and heating loads but can fulfill the heating load, there exists

$$\begin{cases} Q_{R,\max} + S_{\mathrm{HSS}_t} - S_{\mathrm{HSS},\min} < Q_{\mathrm{req}} \\ Q_{R,\max} + S_{\mathrm{HSS}_t} - S_{\mathrm{HSS},\min} \geq Q_{\mathrm{hreq}} \end{cases} \tag{33}$$

Auxiliary boiler don't start and electric chiller start to supply the whole clod load, so $F_{\mathrm{m}} = F_{\mathrm{MT}}$ and

$$E_{\mathrm{ec}} = \frac{Q_{\mathrm{c}} - \eta_{\mathrm{ch}}(Q_{\mathrm{R}} + S_{\mathrm{HSS}_t} - S_{\mathrm{HSS},\min} - Q_{\mathrm{hreq}})}{\eta_{\mathrm{ec}}} \tag{34}$$

Besides, $S_{\mathrm{HSS}_{t+1}} = S_{\mathrm{HSS},\min}$.

c. If the heat produced by the heat recovery system and heat-storage-tank cannot fulfill the heating load, there exists

$$Q_{R,\max} + S_{\mathrm{HSS}_t} - S_{\mathrm{HSS},\min} < Q_{\mathrm{hreq}} \tag{35}$$

Auxiliary boiler start to make up the heating load and electric chiller start to supply the whole clod load, so $E_{\mathrm{ec}} = Q_{\mathrm{c}}/\eta_{\mathrm{ec}}$ and $F_{\mathrm{m}} = F_{\mathrm{MT}} + F_{\mathrm{B}}$ where

$$F_{\mathrm{B}} = \frac{Q_{\mathrm{hreq}} - Q_{\mathrm{R}} - \left(S_{\mathrm{HSS}_t} - S_{\mathrm{HSS},\min}\right)}{\eta_{\mathrm{B}}} \tag{36}$$

Besides, $S_{\mathrm{HSS}_{t+1}} = S_{\mathrm{HSS},\min}$.

Case 2: When the whole cooling and heating loads don't exceed the heat from heat recovery system utilizing the maximum heat power by micro-gas-turbine, there exist

$$Q_{\mathrm{req}} \leq Q_{R,\max} \tag{37}$$

Auxiliary boiler don't start and electric chiller start to supply the whole clod load, so $E_{\mathrm{ec}} = 0$ and $F_{\mathrm{m}} = F_{\mathrm{MT}}$ where

$$F_{\mathrm{MT}} = \frac{Q_{\mathrm{req}}}{\eta_{\mathrm{R}}\,(1 - \eta_{\mathrm{MT}})} \tag{38}$$

Besides, the heat-storage-tank doesn't start where $S_{\mathrm{HSS}_{t+1}} = S_{\mathrm{HSS}_t}$.

D. DESCRPTION AND OPERATION STRATEGY OF SCHP SUPPLY SYSTEM

Herein, a typical SCHP supply system is provided for comparison. It is composed by electric chiller, heating coil and natural gas boiler mainly, shown in Figure 2.

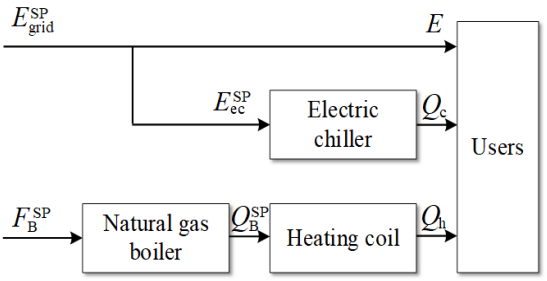

FIGURE 2. Typical SCHP supply system.

For the system in Figure 2, electric power load E is entirely fulfilled by purchasing electricity from power grid. Cooling load Q_{c} is entirely supplied by the electric chiller where the electric power $E^{\mathrm{SP}}_{\mathrm{ec}}$ is purchased from power grid where $E^{\mathrm{SP}}_{\mathrm{ec}} = Q_{\mathrm{c}}/\eta^{\mathrm{SP}}_{\mathrm{ec}}$. Then, $E^{\mathrm{SP}}_{\mathrm{grid}} = E + E^{\mathrm{SP}}_{\mathrm{ec}}$. To fulfill the heating load, the consumed natural gas is $F^{\mathrm{SP}}_{\mathrm{B}} = Q^{\mathrm{SP}}_{\mathrm{B}}/\eta^{\mathrm{SP}}_{\mathrm{B}} = Q_{\mathrm{h}}/\left(\eta^{\mathrm{SP}}_{\mathrm{B}}\eta^{\mathrm{SP}}_{\mathrm{hc}}\right)$.

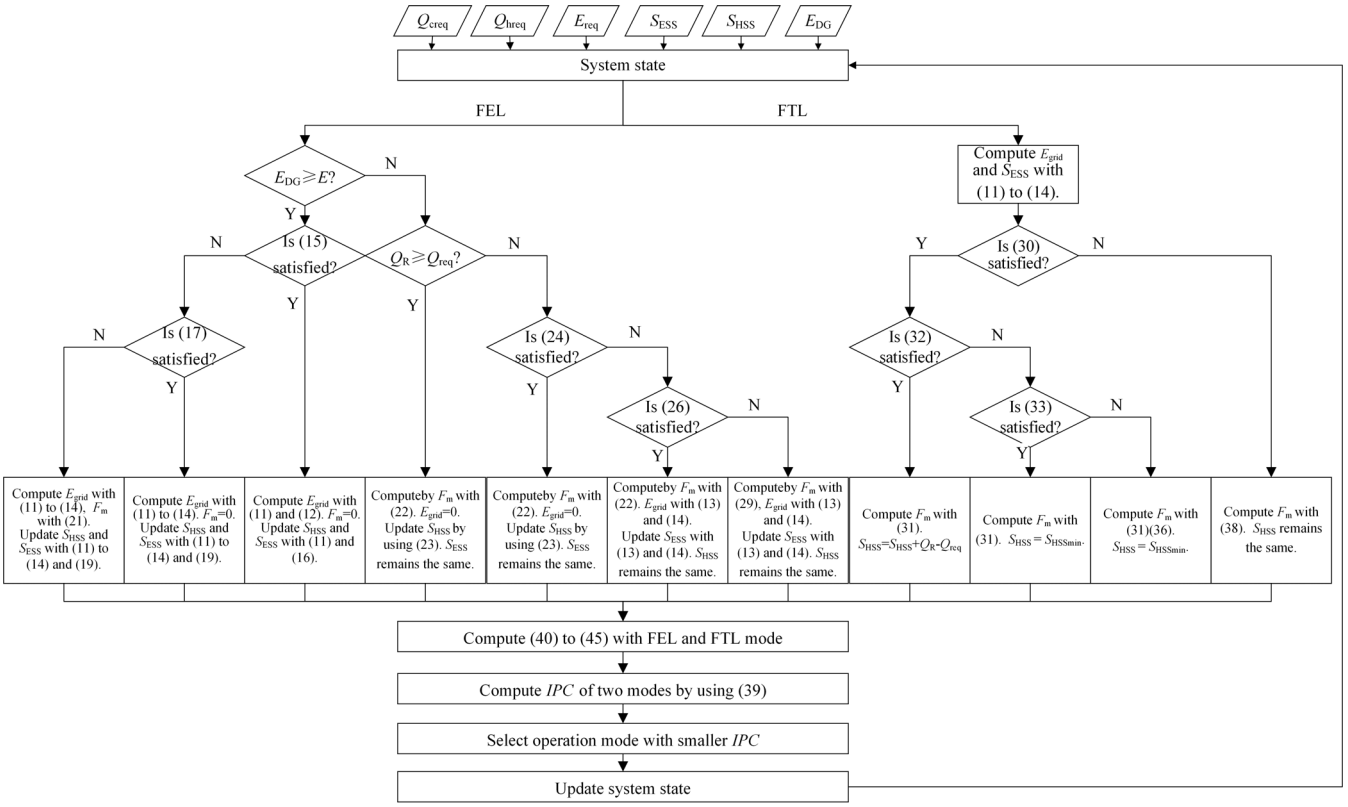

FIGURE 3. Flow chart of the optimal operation strategy.

III. EVALUATION AND OPTIMIZATION

A. COMPREHENSIVE PERFORMANCE EVALUATION

Considering economy, environmental protection and sustainable utilization of multi-energy complementary distributed CCHP system, the comprehensive evaluation index *IPC* is proposed in this paper based on consumption of primary energy *PEC*, carbon dioxide emission *CDE* and operation cost *COST*, defined by

$$IPC = \omega_1 \frac{PEC_{\mathrm{CCHP}}}{PEC_{\mathrm{SCHP}}} + \omega_2 \frac{CDE_{\mathrm{CCHP}}}{CDE_{\mathrm{SCHP}}} + \omega_3 \frac{COST_{\mathrm{CCHP}}}{COST_{\mathrm{SCHP}}} \tag{39}$$

where ω_1, ω_2 and ω_3 are weighting coefficients. Their constraints are $0 \leq \omega_1, \omega_2, \omega_3 \leq 1$ and $\omega_1 + \omega_2 + \omega_3 = 1$. Considering the relative importance of each terms, the weights are chosen to be equal, which can make the results nearly as good as those unequal weighting methods [19]. Besides, the following constraints exist

$$PEC_{\mathrm{CCHP}} = E_{\mathrm{grid}}^{\mathrm{CCHP}} \sigma_e + F_m \sigma_f \tag{40}$$

$$PEC_{\mathrm{SCHP}} = E_{\mathrm{grid}}^{\mathrm{SCHP}} \sigma_e + F_b^{\mathrm{SCHP}} \sigma_f \tag{41}$$

$$CDE_{\mathrm{CCHP}} = E_{\mathrm{grid}}^{\mathrm{CCHP}} \mu_e + F_m \mu_f \tag{42}$$

$$CDE_{\mathrm{SCHP}} = E_{\mathrm{grid}}^{\mathrm{SCHP}} \mu_e + F_b^{\mathrm{SCHP}} \mu_f \tag{43}$$

$$COST_{\mathrm{CCHP}} = E_{\mathrm{grid}}^{\mathrm{CCHP}} C_e + F_m C_f + F_m \mu_f C_c \tag{44}$$

$$COST_{\mathrm{SCHP}} = E_{\mathrm{grid}}^{\mathrm{SCHP}} C_e + F_{\mathrm{boiler}}^{\mathrm{SCHP}} C_f + F_b^{\mathrm{SCHP}} \mu_f C_c \tag{45}$$

where F_m is the total fuel consumed by the CCHP system; σ_f is the conversion coefficient of primary energy to per consumed kilowatt-hour fuel; μ_f (g/KWh) is the carbon dioxide emission of per kilowatt-hour fuel; C_f is the price of per kilowatt-hour fuel. $E_{\mathrm{grid}}^{\mathrm{CCHP}}$ is the purchased electricity by the CCHP system; σ_e is the conversion coefficient of primary energy to per kilowatt-hour electricity purchased from power grid; μ_e (g/KWh) is the carbon dioxide emission of per kilowatt-hour electricity; C_e is the price of per kilowatt-hour electricity. C_c is the tax of carbon dioxide emission.

B. OPTIMAL OPERATION STRATEGY

If the multi-energy complementary distributed CCHP system structure has been determined, the consumed fuel, purchased electricity from power grid and surplus power supply to grid are also different at certain time instant to fulfill the heating, cooling and electric power loads using different operation modes. Thus, at certain time instant, to find the optimal operation mode is very important, which is also a precondition to maximize the benefit. Herein, to determine the optimal operation mode, the decision strategy is set as following: the mode with higher *IPC* is taken as the optimal operation mode under the FTL mode or FEL mode. The decision-making process of this strategy is shown in Figure 3.

IV. SIMULATION AND VALIDATION

A commercial building in Beijing, China (40.08N, 116. 31E) is selected for research. This three-floor building covers a

total area of 4050 square meters. There are 300 restaurants and 1050 offices on the first floor and 1350 rooms on the second and third floors. There are limited renewable energy sources around this building, so the solar power station with 20KWp capacity is installed.

Using EnergyPlus software, energy consumption of the whole building is analyzed. Its annual demand including cooling, heating and electric power loads can be simulated and calculated. According to the forecasting method proposed by Zhang [20], the photovoltaic power, cooling, heating and electric power load on typical days of this CCHP system can be forecasted.

TABLE 1. Efficiency values of equipment.

System	Parameter	Symbol	Value
CCHP	Efficiency of micro gas turbine	η_{MT}	0.29
	Efficiency of Waste Heat Boiler	η_{R}	0.8
	Efficiency of Absorption Refrigerator	η_{ch}	0.7
	heat exchanger efficiency	η_{hc}	0.8
	Peak Boiler Efficiency	η_{B}	0.8
SCHP	Efficiency of Electric Refrigerator	η_{ec}	3
	Efficiency of Electric Refrigerator	η^{SP}_{ec}	3
	Efficiency of Absorption Refrigerator	η^{SP}_{hc}	0.8
	Peak Boiler Efficiency	η^{SP}_{B}	0.8

TABLE 2. Preset parameters in evaluation indexes.

Parameters	Symbol	Value
Tax of carbon dioxide emission	C_c	0.00002 (Y/g)
Carbon dioxide emission of per kilowatt-hour electricity and fuel	μ_e	968(g/kWh)
	μ_f	220(g/kWh)
Conversion coefficient of primary energy to per kilowatt-hour electricity and fuel	σ_e	3.336
	σ_f	1.047

The maximum output power of micro-gas-turbine in the system is 65 kWp and its heat-power ratio is 2.45. The rated capacities of battery and heat-storage-tank are both 20 kWh. Their initial states are both 50% of rated capacities and their minimum capacities are 10% of rated capacities. Efficiency values of equipment in the CCHP system and SCHP system are listed in Table 1. Preset parameters in the evaluation indexes are shown in Table 2. Interactive electricity price between the CCHP or SCHP system and the power grid is shown in Table 3.

For different seasons such as spring, summer and winter, three typical days are selected for validation. Their cooling, heating and electric power loads and renewable energy output are shown in Figure 4. In different seasons, the electric loads are very similar. In summer, the cooling load increases significantly, while the heating load is very low. In winter, the heating load is very high whereas the cooling load is low.

TABLE 3. Preset parameters in evaluation indexes.

Direction	Time Period	Electricity Price (RMB)
Purchased from grid	Valley: 23:00-06:59	0.3658
	General: 07:00-09:59, 15:00-15:59, 17:00-17:59, 21:00-22:59	0.8595
	Peak: 10:00-10:59, 13:00-14:59, 18:00-20:59	1.3782
	Peak: 11:00-12:59, 16:00-16:59	1.5065
Sold to grid	Full time: 0:00-23:59	0.7098

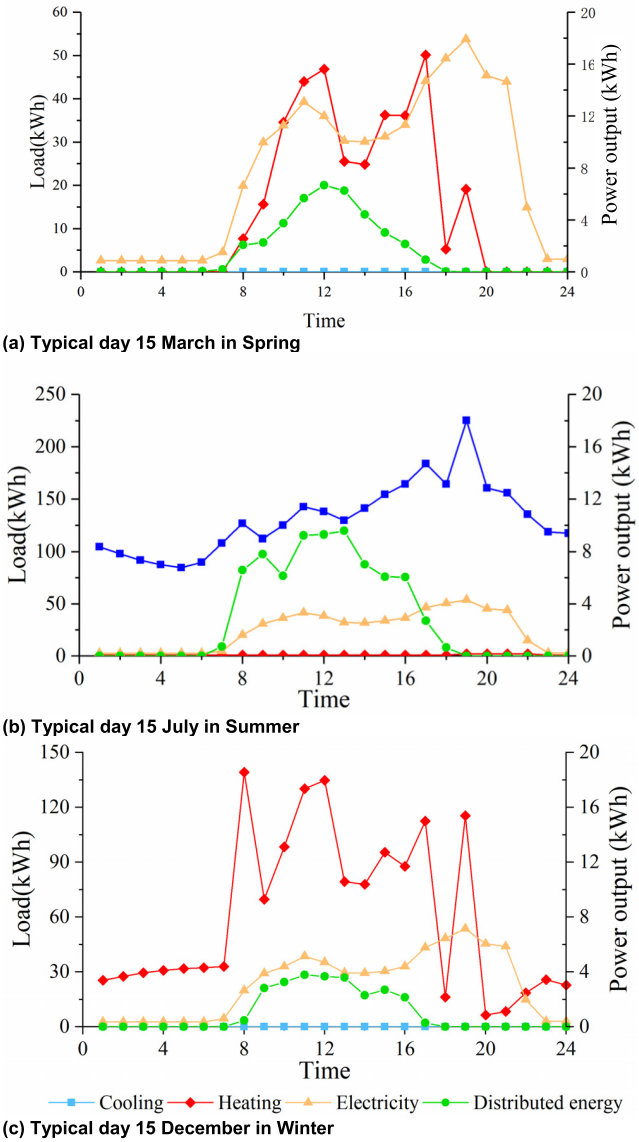

FIGURE 4. Cooling, heating and electric loads and renewable energy output of typical days.

In spring, the heating load is higher than the cooling load. On a daily scale, the loads during the day is higher than that at night. Because renewable energy output is directly affected by solar irradiance, average power in summer is the highest and the available period is the longest, which is contrary to that in winter. During the day, renewable energy output increases gradually with the rise of the sun and decreases gradually after the maximum output at noon.

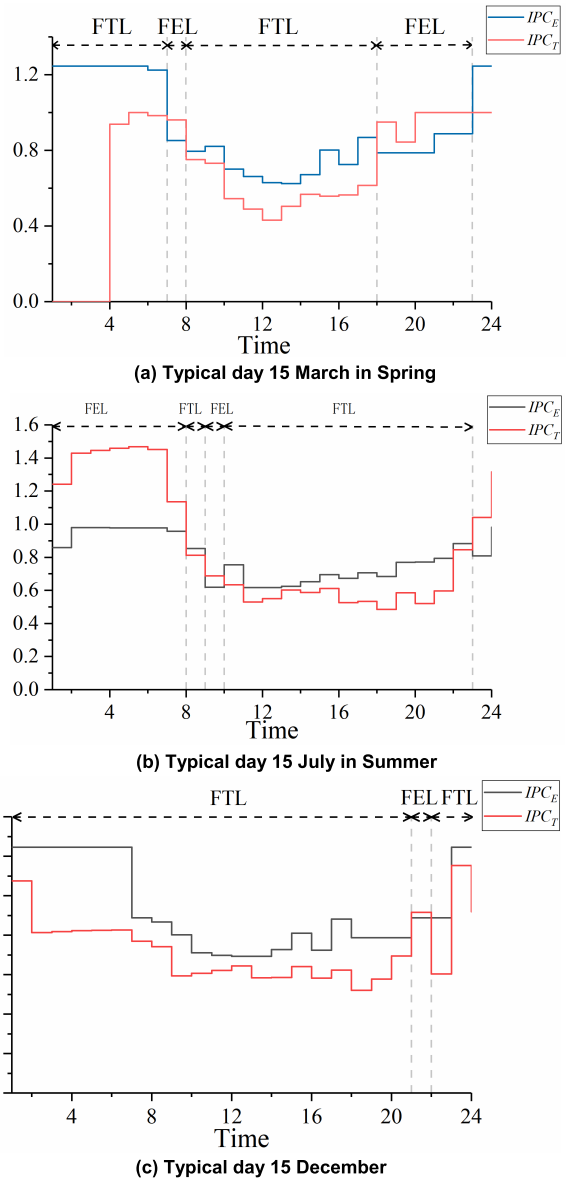

FIGURE 5. Optimal operation strategies of typical days.

Based on the calculation of *IPC*, the optimal operation strategies for each hour of typical days are shown in Figure 5 where IPC_E means IPC index for electric load and IPC_T means IPC index for thermal load.

Based on the above optimal operation strategies, the changing of reserve energy per hour in the battery and heat-storage-tank of the CCHP system are shown in Figure 6. When the system has surplus energy, priority should be given to battery and heat-storage-tank to avoid waste of energy. When the system cannot meet the user loads, priority should be given to energy storage units to fulfill user demand and improve economy of the CCHP system. It is also a self-adjusting means to face user demand changes, improve system reliability and reduce external dependence.

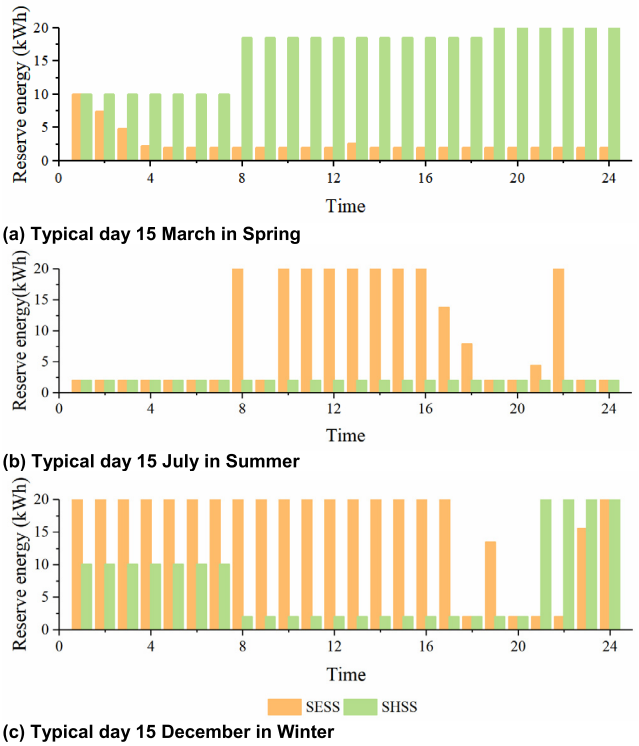

FIGURE 6. Changing of reserve energy per hour on different typical days based on optimal operation strategies.

The fuels consumed by auxiliary boiler and micro-gas-turbine on typical days are shown in Figure 7.

Interactively transmitted electricity with the grid on typical days is shown in Figure 8. When the transmitted electricity has positive value, it suggests that the sum of power generation capacity and battery capacity in the CCHP system are not enough to meet the electric power loads of user. The CCHP system has to purchase electricity from power grid. When the transmitted electricity has negative value, it suggests that the power generation capacity in the CCHP system is enough to meet the electric power loads of user and the battery has been fully charged to its maximum capacity. Then, the surplus electric power is sold to the power grid.

For the three typical days, operation performance of the CCHP system using optimal operation strategy is compared with that of the CCHP system under FTL mode and the SCHP system. The evaluation indexes are shown in Table 4.

It can be seen that the optimal operation strategy proposed in this paper is superior to the SCHP system in terms of the indexes such as *PEC*, *CDE*, *COST* and *IPC*. Compared with

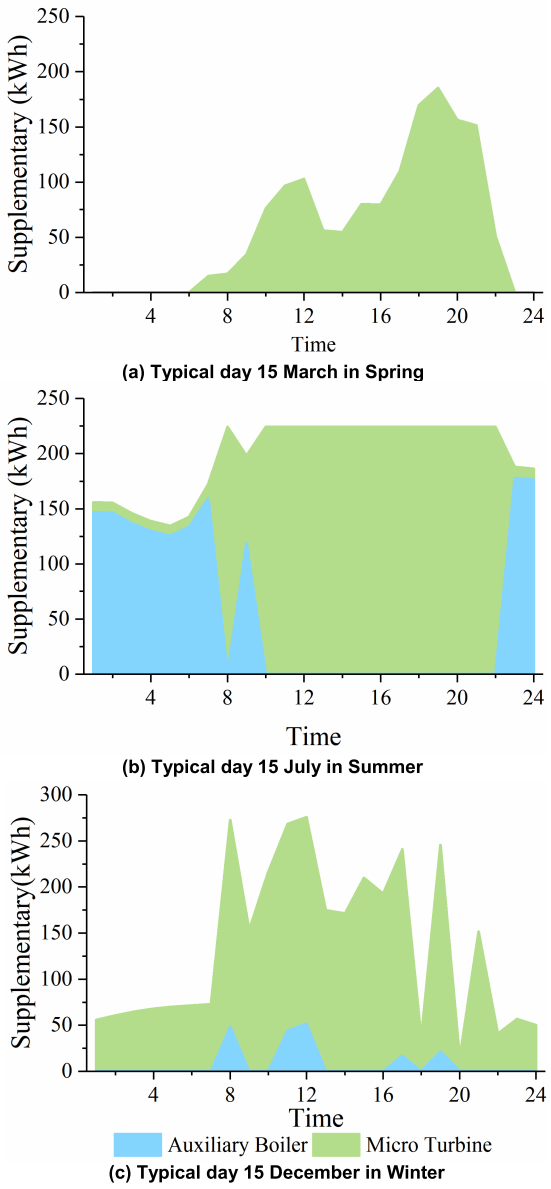

FIGURE 7. Consumed fuels on typical days.

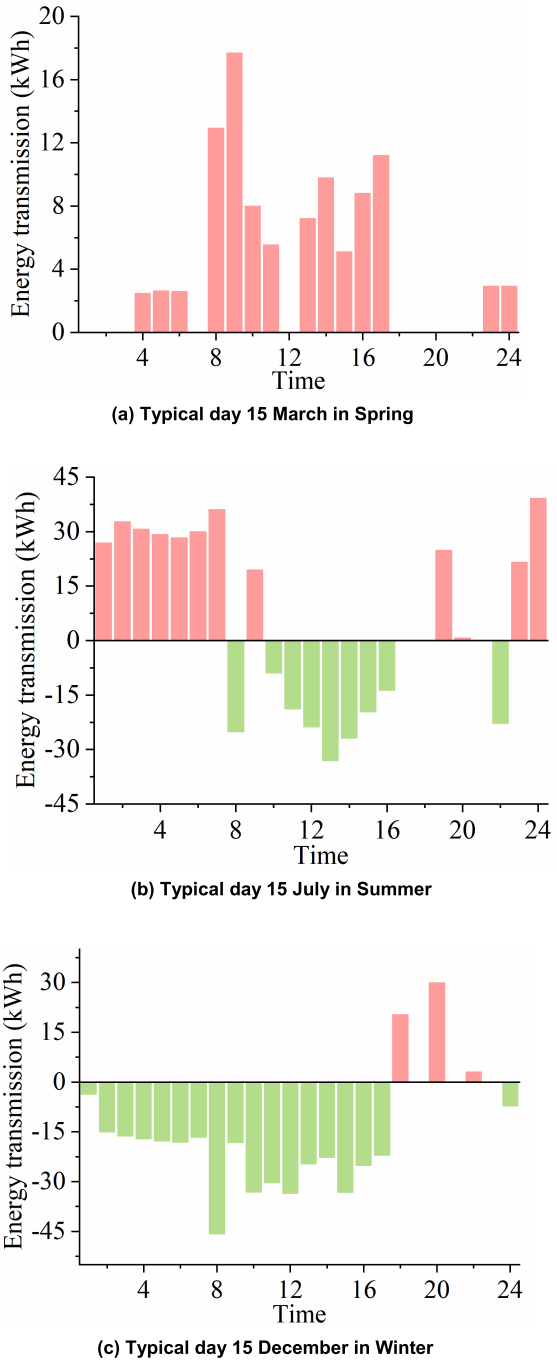

FIGURE 8. Interactively transmitted electricity with grid on typical days.

the FTL mode of CCHP system, although some performance indexes are slightly worse, comprehensive performance of the optimal model of CCHP system is superior to that of the single mode.

If electric power load keep constant, with the addition of renewable energy, the required output power from micro-gas-turbine becomes smaller, reducing primary energy consumption and operation cost to a certain extent. In spring and autumn seasons, the cooling and heating loads are relatively low and the carbon dioxide emission has been reduced by 6.5%.

Adding energy storage in the CCHP system can reduce primary energy consumption and carbon dioxide emission. Especially in winter, the two indicators are decreased by nearly 10%, significantly improving the environmental protection. Since priority is given to the CCHP system itself to fill the user loads instead of purchasing electricity from power grid, the whole system reliability is improved although sacrificing partial economy.

For the summer with high demand of cooling load, the addition of electric chiller in the CCHP system can efficiently raise the comprehensive performance while reducing the primary energy consumption by 28.8% and the carbon

TABLE 4. Performance evaluation of different operation modes.

Date	System	*PEC*	*CDE*	*COST*	*IPC*
15 March	SCHP	2438.082979	662184.1605	775.3649155	NULL
	FTL mode of CCHP	1781.579121	453197.6112	489.1373491	0.681991852
	Optimal mode of CCHP	1858.898364	394187.7517	348.6704769	0.602470814
15 July	SCHP	5496.213513	1591158.043	1736.144628	NULL
	FTL mode of CCHP	5594.282122	1182257.325	532.9539272	0.689276846
	Optimal mode of CCHP	4457.60656	1028828.262	731.8327857	0.626383564
15 December	SCHP	4217.413015	1034030.742	1107.783198	NULL
	FTL mode of CCHP	3551.45877	770712.9937	436.4928129	0.660488685
	Optimal mode of CCHP	3139.214573	667778.5439	601.8038276	0.644466001

TABLE 5. Performance evaluation of additional components.

Date	System	*PEC*	*CDE*	*COST*	*IPC*
15 March	Basic CCHP	2020.626	430318.6	377.1743	0.655024
	With renewable energy	1887.065	402242.4	351.8771	0.611755
	With energy storage	1993.938	422574.6	374.2479	0.646219
	With electric chiller	2020.626	430318.6	377.1743	0.655024
15 July	Basic CCHP	6580.589	1382740.7	731.9081	0.829293
	With renewable energy	6530.442	1372203.8	705.4698	0.818969
	With energy storage	6570.119	1380540.7	737.0221	0.829179
	Electric chiller	4682.989	1079464.1	730.1602	0.650339
15 December	Basic CCHP	3523.989	740475.27	488.9743	0.664361
	With renewable energy	3504.340	736346.6	480.8172	0.659023
	With energy storage	3165.403	673281.6	606.7665	0.649803
	With electric chiller	3523.989	740475.2	488.9743	0.664361

dioxide emission by 21.9% and keeping the operation cost unchanged.

V. CONCLUSION

In this paper, optimal operation of a multi-energy complementary distributed CCHP system is deeply studied and applied on a commercial building in Beijing. Executable optimal strategies are presented for the optimal operation of this complex system with many energy-source and energy-conversion devices. After comparison with a SCHP supply system, the multi-energy system has better profit and lower cost. It fully shows effectiveness of the optimal strategy for this multi-energy complementary distributed CCHP system of a commercial building.

REFERENCES

[1] M. Chahartaghi and M. Sheykhi, "Energy, environmental and economic evaluations of a CCHP system driven by Stirling engine with helium and hydrogen as working gases," *Energy*, vol. 174, pp. 1251–1266, May 2019.
[2] P. Chen, Y. Lan, D. Wang, W. Wang, W. Liu, Z. Chong, and X. Wang, "Optimal planning and operation of CCHP system considering renewable energy integration and seawater desalination," *Energy Procedia*, vol. 158, pp. 6490–6495, Feb. 2019.
[3] Y. Li, W. Yang, P. He, C. Chen, and X. Wang, "Design and management of a distributed hybrid energy system through smart contract and blockchain," *Appl. Energy*, vol. 248, pp. 390–405, Aug. 2019.
[4] X. P. Chen, N. Hewitt, Z. T. Li, Q. M. Wu, X. Yuan, and T. Roskilly, "Dynamic programming for optimal operation of a biofuel micro CHP-HES system," *Appl. Energy*, vol. 208, pp. 132–141, Dec. 2017.
[5] F. A. Boyaghchi and P. Heidarnejad, "Thermoeconomic assessment and multi objective optimization of a solar micro CCHP based on organic rankine cycle for domestic application," *Energy Convers. Manage.*, vol. 97, pp. 224–234, Jun. 2015.
[6] D. Wu, J. Zuo, Z. Liu, Z. Han, Y. Zhang, Q. Wang, and P. Li, "Thermodynamic analyses and optimization of a novel CCHP system integrated organic Rankine cycle and solar thermal utilization," *Energy Convers. Manage.*, vol. 196, pp. 453–466, Sep. 2019.
[7] F. Fang, L. Wei, J. Liu, J. Zhang, and G. Hou, "Complementary configuration and operation of a CCHP-ORC system," *Energy*, vol. 46, no. 1, pp. 211–220, 2012.
[8] J.-J. Wang, Y.-Y. Jing, and C.-F. Zhang, "Optimization of capacity and operation for CCHP system by genetic algorithm," *Appl. Energy*, vol. 87, no. 4, pp. 1325–1335, 2010.
[9] W. Lin, X. Jin, Y. Mu, H. Jia, X. Xu, X. Yu, and B. Zhao, "A two-stage multi-objective scheduling method for integrated community energy system," *Appl. Energy*, vol. 216, pp. 428–441, Apr. 2018.
[10] H. An, W. Lin, X. Jin, Q. Zhou, and B. Cen, "Stochastic multi-objective scheduling approach for integrated community energy system," in *Proc. IEEE Int. Conf. Energy Internet*, Beijing, China, May 2018, pp. 321–325.
[11] W. Wang, S. Jing, Y. Sun, J. Liu, Y. Niu, D. Zeng, and C. Cui, "Combined heat and power control considering thermal inertia of district heating network for flexible electric power regulation," *Energy*, vol. 169, pp. 988–999, Feb. 2019.
[12] X. Zhu, X. Zhan, H. Liang, X. Zheng, Y. Qiu, J. Lin, J. Chen, C. Meng, and Y. Zhao, "The optimal design and operation strategy of renewable energy-CCHP coupled system applied in five building objects," *Renew. Energy*, to be published.
[13] S. Lin, C. Yang, W. Song, and Z. Feng, "Analysis of capacity and control strategy for distributed energy system with hybrid energy storage system," in *Proc. Int. Conf. Smart Grid Clean Energy Technol.*, Kajang, Malaysia, May/Jun. 2018, pp. 84–88.
[14] M. Liu, Y. Shi, and F. Fang, "Optimal power flow and PGU capacity of CCHP systems using a matrix modeling approach," *Appl. Energy*, vol. 102, pp. 794–802, Feb. 2013.
[15] X. Wang, X. Shi, H. Zhang, and F. Wang, "Multi-objective optimal dispatch of wind-integrated power system based on distributed energy storage," in *Proc. 43rd Annu. Conf. IEEE Ind. Electron. Soc.*, Beijing, China, Oct./Nov. 2017, pp. 2788–2792.
[16] S. Esmaeili and S. Jadid, "Economic-environmental optimal management of smart residential micro-grid considering CCHP System," *Electr. Power Compon. Syst.*, vol. 46, nos. 14–15, pp. 1592–1606, 2018.
[17] W. Lin, X. Jin, Y. Mu, H. Jia, X. Xu, and X. Yu, "Multi-objective optimal hybrid power flow algorithm for integrated community energy system," *Energy Procedia*, vol. 105, pp. 2871–2878, May 2017.
[18] W. Wang, Z. Liang, Y. Wang, and Y. Zhu, "Optimal configuration of multi-energy complementary distributed energy system," in *Proc. Conf. Ser. Earth Environ. Sci.*, vol. 189, 2018, pp. 52–85.
[19] R. M. Dawes and B. Corrigan, "Linear models in decision making," *Psychol. Bull.*, vol. 81, no. 2, pp. 95–106, 1974.
[20] X. Zhang, F. Fang, and J. Liu, "Weather-classification-MARS-Based photovoltaic power forecasting for energy imbalance market," *IEEE Trans. Ind. Electron.*, vol. 66, no. 11, pp. 8692–8702, Nov. 2019.

QINGHUA WANG received the M.S. degree in control theory and engineering from North China Electric Power University, Beijing, China. He is currently pursuing the Ph.D. degree in thermal power engineering with the School of Energy, Power and Mechanical Engineering. His research interests include operation, planning, and optimization of combined cycle energy systems.

JIZHEN LIU was born in China, in 1951. He received the M.S. degree in power plant engineering from the Graduate Faculty of North China Electric Power Institute, Beijing, China, in 1982. He is currently an Academician with the China Engineering Academy, and a Professor with the State Key Laboratory of Alternate Electrical Power System With Renewable Energy Sources, North China Electric Power University. His research interest includes large-scale renewable energy integration.

YANG HU received the Ph.D. degree in thermal power engineering from the School of Energy, Power and Mechanical Engineering, in 2015. He is currently with the School of Control and Computer Engineering, North China Electric Power University, Beijing, China. His research interests include control and data analysis of renewable energy power systems, virtual power plant, microgrids, and integrated energy systems.

XIAONING ZHANG received the M.S. degree in control theory and engineering from North China Electric Power University, Beijing, China, in 2019, where he is currently pursuing the Ph.D. degree in control science and engineering with the School of Control and Computer Engineering. His research interests include the forecasting of distributed renewable energy and deep learning applications in power systems.